



# Zeolite-FAU-templated N-Carbons for Oxygen Reduction Reaction.

Leonardo L. dos Santos 1\*, Aurélien Habrioux 2, Sibele B. C. Pergher 1, Alexander Sachse 2.

- <sup>1</sup> Federal University of Rio Grande do Norte, Laboratório de Peneiras Moleculares (LABPEMOL) IQ 2, st. Senador Salgado Filho 3000, 59078-970 Natal/RN Brazil.
- <sup>2</sup> Université de Poitiers, Institut de Chimie des Milieux et Matériaux de Poitiers (IC2MP) UMR 7285 CNRS, UFR SFA, Bât. B27, 4 rue Michel Brunet, TSA 51106, 86073 Poitiers Cedex 9 France.
- \* leo.leandro25@gmail.com

#### **Abstract**

ABSTRACT - Zeolite-templated carbons (ZTCs) doped with carbon (C-ZTC) and carbon/nitrogen (CN-ZTC) were synthesized using ethylene and acetonitrile as respective precursors. These materials were comprehensively characterized through nitrogen adsorption at 77 K, scanning electron microscopy (SEM), X-ray diffraction (XRD), thermogravimetric analysis (TGA), Raman spectroscopy, and X-ray photoelectron spectroscopy (XPS). The CN-ZTC exhibited a notably high nitrogen incorporation (C/N ratio of 12.5) and a less condensed carbon framework compared to its nitrogen-free counterpart. A decreased micropore volume in CN-ZTC was attributed to the presence of graphene-like carbon domains formed on the outer surface of the ZTC, which enhanced its electronic conductivity. Catalysts derived from CN-ZTC demonstrated exceptional oxygen reduction reaction (ORR) performance, with a half-wave potential of 0.81 V versus RHE and pronounced selectivity toward hydroxyl formation.

Keywords: Zeolite Templated Carbons, Faujasite, Nitrogen functionalization, Oxygen reduction reactions, Graphene

#### Introduction

Zeolite-Templated Carbons (ZTCs) have garnered considerable attention due to their unique combination of high electrical conductivity and well-defined microporosity, making them suitable for a range of applications, including gas storage and electrochemical energy conversion. These materials are synthesized by carbonizing organic precursors within the microporous structure of a zeolite template, followed by template removal, yielding a negative replica of the original zeolite framework. Although the exact atomic arrangement of ZTCs remains under discussion, structural models generally fall into closed strut or open blade configurations. Carbon nanostructures such as ZTCs are particularly promising for use in fuel cell electrodes, especially for the oxygen reduction reaction (ORR), a key process at the cathode of hydrogen fuel cells. In alkaline environments, the ORR ideally proceeds via a four-electron pathway producing hydroxide ions, yet often follows a less efficient two-electron mechanism involving peroxide intermediates [1,2].

Platinum remains the benchmark catalyst for ORR due to its ability to favor the four-electron path. However, its high cost, limited availability, vulnerability to CO poisoning, and poor long-term stability – due to agglomeration and degradation – pose significant barriers to large-scale deployment. In this context, the development of metal-free electrocatalysts has emerged as a compelling alternative. Among these, graphene-based materials functionalized with heteroatoms like nitrogen or phosphorus have been explored, though post-synthetic doping generally results in

low heteroatom incorporation and modest catalytic performance [3,4].

More recently, a one-step strategy has been demonstrated, using nitrogen-containing precursors such as acetonitrile or pyrrole during ZTC synthesis, which allows simultaneous framework formation and nitrogen doping. This method yields materials with integrated active sites and improved conductivity, despite typically low nitrogen content (~4 Pioneering work by Quílez-Bermejo collaborators showed that such materials can achieve significant ORR activity, with half-wave potentials approaching 0.77 V vs. RHE under alkaline conditions. Nonetheless, synthesis conditions - particularly hightemperature treatments - can lead to partial degradation of the zeolite template (e.g., via dealumination above 600 °C), which may hinder framework condensation and impair conductivity [5].

In this study, we investigate and compare the ORR performance of a purely carbon-based ZTC with that of a nitrogen-doped ZTC synthesized directly from acetonitrile. The latter exhibited both a higher nitrogen content and enhanced electronic conductivity, resulting in markedly improved catalytic activity for the ORR.

# Experimental

Materials

All chemicals were procured from commercial suppliers and used without further purification. Acetonitrile (anhydrous, 99.8%), calcium nitrate tetrahydrate (99%),



sodium bicarbonate (99%), and boric acid (99%) were obtained from Sigma-Aldrich. Hydrofluoric acid (49% aqueous solution) and hydrochloric acid (37%) were purchased from Fisher Scientific. NaX zeolite was acquired from Axence, while ethylene (>99.99%) and nitrogen (99.995%) were supplied by Air Liquide. Commercial Pt/C (E-tek) was used as received.

# Cation exchange of NaX zeolite

To prepare the calcium-exchanged zeolite, 1 g of NaX was suspended in 100 mL of a 0.5 M aqueous solution of Ca(NO<sub>3</sub>)<sub>2</sub> and stirred at 80 °C for 2 hours. The solid was filtered, extensively washed with deionized water, and dried at 80 °C. This ion-exchange process was repeated twice more, and the resulting material was then calcined in air at 550 °C for 6 hours.

### Synthesis of C- and CN-ZTC

The Ca<sup>2+</sup>-exchanged zeolite was placed in a quartz tubular reactor with a fritted base and pretreated at 150 °C under a nitrogen flow (150 mL min<sup>-1</sup>) for 1 hour to remove physisorbed water. The temperature was then increased to 790 °C, and after 1 hour, a gas mixture of 6.67 vol% ethylene in nitrogen was introduced for 4 hours to initiate carbon deposition. Subsequently, the system was heated to 890 °C for 2 hours under nitrogen to complete the pyrolysis. After cooling to room temperature, the composite was treated first with concentrated HCl at 80 °C for 2 hours, then with 49 wt% HF at room temperature for 4 hours to dissolve the zeolite. Fluoride residues were neutralized by sequential addition of saturated H<sub>3</sub>BO<sub>3</sub> and NaHCO<sub>3</sub> aqueous solutions (60 mL each). After stirring for 1 hour at room temperature, the carbonaceous material was filtered, thoroughly washed with hot distilled water, and dried overnight at 80 °C, yielding the final C-ZTC. For CN-ZTC synthesis, the same procedure was followed up to the activation stage at 790 °C. Instead of ethylene, acetonitrile was introduced via syringe pump (2.5 mL h<sup>-1</sup>) for 4 hours under nitrogen flow. Following this, the reactor was heated to 890 °C for 2 hours before cooling. The post-synthesis treatment and purification steps remained unchanged, leading to the final CN-ZTC product.

#### Characterization

Material characterization included structural packing density (SPD) determination by thermogravimetric analysis (TGA, SDT Q600) under synthetic air up to 900 °C (10 °C min<sup>-1</sup>), quantifying carbonaceous content per gram of zeolite. Textural properties were assessed via N<sub>2</sub> physisorption at 77 K (Micromeritics 3Flex) after degassing at 350 °C for 12 h, with surface area and micropore volume calculated using the t-plot method and NLDFT for pore size distribution. X-ray diffraction (PANalytical Empyrean, CuKα) was performed in the 5–50° 2θ range. Elemental



composition (C, H, N, O) was analyzed via CHNS elemental analysis (Flash EA 1112/2000), and metal content via ICP-OES (Perkin Elmer Optima 2000 DV). SEM imaging (JEOL JSM-790CF) was used to examine morphology, while Raman spectroscopy (514 nm excitation, Labram HR 800-UV) provided insight into structural disorder. XPS (Kratos Axis Ultra DLD, Al K $\alpha$ , 1486.6 eV) was employed for surface composition and chemical state analysis (C1s, N1s, O1s), with spectra fitted using CasaXPS software (version 2.3.24). Electrical conductivity was measured by impedance spectroscopy (Solartron SI 1287/1260) using powdered samples pressed between gold electrodes, with resistance values taken at 0° phase shift and normalized to graphite.

#### Results and discussion

The NaX zeolite used as a template exhibits a Si/Al ratio of 1.13 and a Ca/Al ratio of 0.49, with its microporous nature confirmed by a type I nitrogen physisorption isotherm and a micropore volume of 0.31 cm<sup>3</sup> g<sup>-1</sup> (Fig. 1). XRD analysis confirms the presence of the FAU phase, and SEM images show the characteristic bipyramidal morphology.

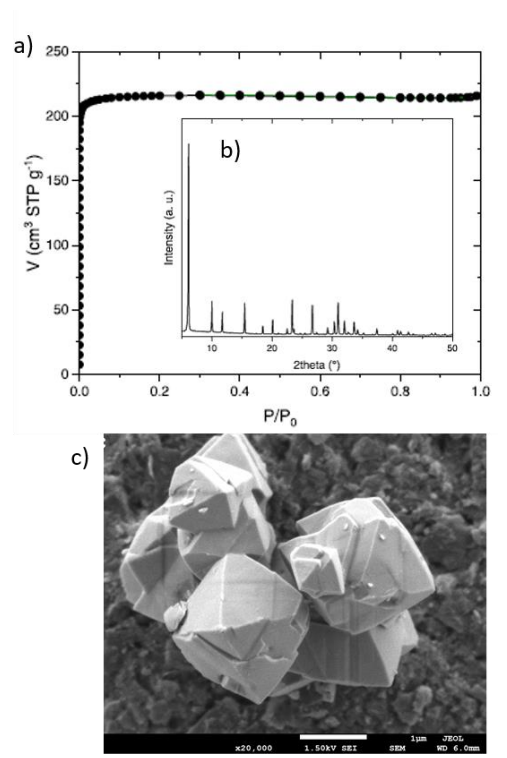


**Fig. 1.** Nitrogen physisorption isotherm at 77 K (a), XRD powder pattern (b) and SEM image of the zeolite X template.

Upon carbonization, both ethylene and acetonitrile precursors fully occlude the zeolite micropores. From thermogravimetric data, the structural packing densities (SPD) were determined to be  $0.30 \, \mathrm{gC} \, \mathrm{gZ^{-1}}$  for the C-hybrid



and 0.34 gC gZ<sup>-1</sup> for the CN-hybrid (Fig. 2a), suggesting the formation of additional carbon species on the external surfaces in the CN-hybrid. The CN-hybrid also exhibits a delayed combustion profile with a heat release maximum at 560 °C, compared to 475 °C for the C-hybrid, likely due to nitrogen incorporation and a less condensed carbon network. The heat of combustion further supports this distinction, with values of 5.7 and 11.7 kJ g<sup>-1</sup> for the C- and CN-hybrids, respectively.

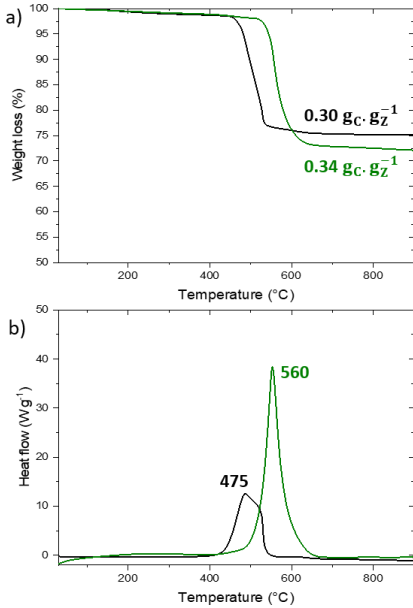


Fig. 2. TGA weight loss curves (a) and heat flow as a function of the temperature (b) of the C-hybrid (black) and CN-hybrid (green).

After template removal, both C-ZTC and CN-ZTC retain the original zeolite morphology, as evidenced by SEM images (Fig. 3). However, nitrogen adsorption data reveal significant textural differences (Fig. 4a): while both display type I isotherms, C-ZTC has a micropore volume of  $1.101 \, \mathrm{cm^3 \, g^{-1}}$  – roughly twice that of CN-ZTC (Table 1). NLDFT analysis shows similar pore size distributions (Fig. 4b), indicating that both precursors replicate the zeolite structure effectively. In XRD patterns, C-ZTC presents a peak at  $6.4^{\circ}$  2 $\theta$ , indicating structural order, while CN-ZTC exhibits a broader signal and an additional peak at ~24° 2 $\theta$ , attributed to (002) stacking of graphene-like layers (Fig. 4c), which may reduce microporosity and enhance conductivity.



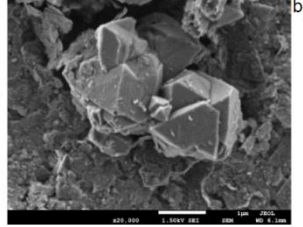
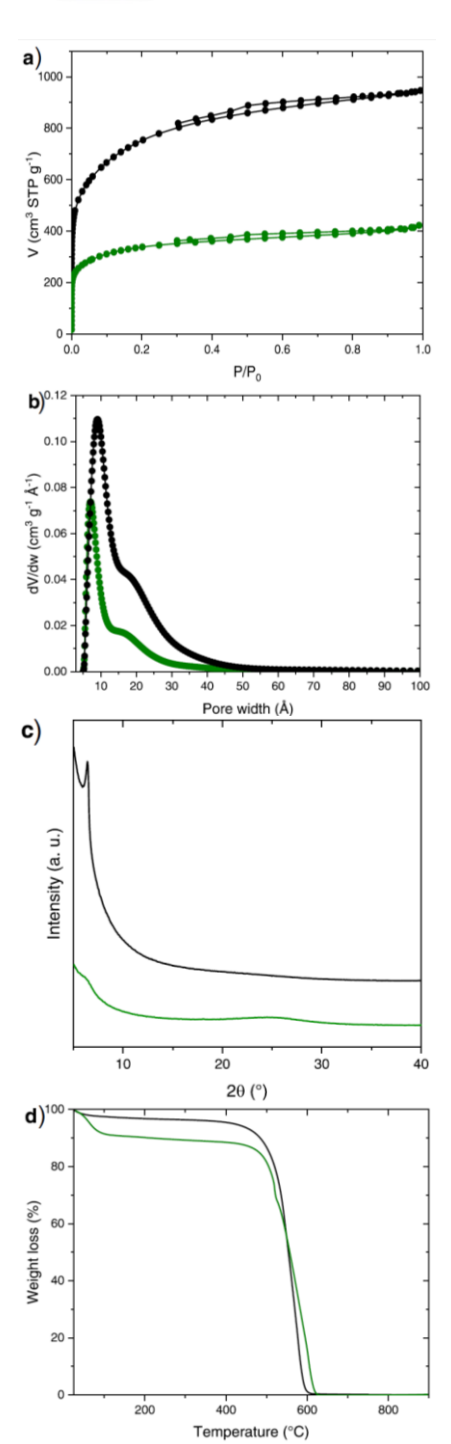


Fig. 3. SEM images of C-ZTC (a) and CN-ZTC (b).





**Fig. 4.** N<sub>2</sub> physisorption isotherms at 77 K (a), NLDFT pore size distribution (b), XRD powder patterns (c), and TGA weight loss curves (d) of C-ZTC (black) and CN-ZTC (green).

Tab. 1. Chemical and textural properties of C-ZTC and CN-ZTC

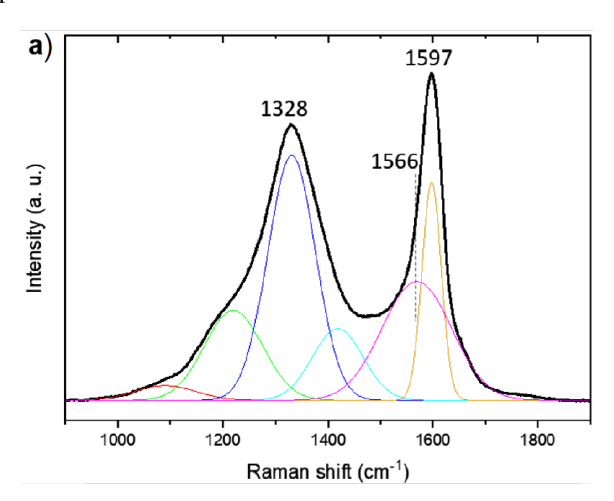
Tab. 1. Chemical and textural properties of C-21C and CN-21C.							
		SPD	$V_{\text{micro}}$	$S_{BET}$	C/H	C/N	NC
ı		(gCgZ <sup>-1</sup> )	(cm <sup>3</sup> g <sup>-1</sup> )	$(m^2g^{-1})$			(S.m <sup>-1</sup> )*
ı	C-ZTC	0.30	1.01	2748	7.4	ı	0.05
I	CN-ZTC	0.34	0.48	1230	3.5	12.9	0.35

<sup>\*</sup>NC = Normalized conductivity by the value recorded for graphite.



TGA confirms complete combustion of both samples by 660 °C, with no residual inorganic content (Fig. 4d). CN-ZTC shows a higher water content (mass loss <100 °C), likely due to increased surface polarity from nitrogen functionalities. Elemental analysis reveals a higher C/H ratio in C-ZTC (7.4 vs. 3.5), indicating a more aromatic and condensed structure, Table 1.

Raman spectra (Fig. 5) further support this: CN-ZTC shows a blue shift in both G (1604 vs. 1597 cm<sup>-1</sup>) and D bands (1348 vs. 1328 cm<sup>-1</sup>), and a higher D/G intensity ratio (1.3 vs. 1.1), suggesting more disorder and edge sites. The lateral crystallite size (La) is smaller for CN-ZTC (3.49 nm) compared to C-ZTC (4.11 nm), consistent with its lower structural condensation. Additional broadening and asymmetry in the CN-ZTC Raman spectrum, including a shoulder near 1566 cm<sup>-1</sup>, indicates the presence of sp<sup>3</sup>-hybridized carbon, likely associated with pyrrolic nitrogen species.



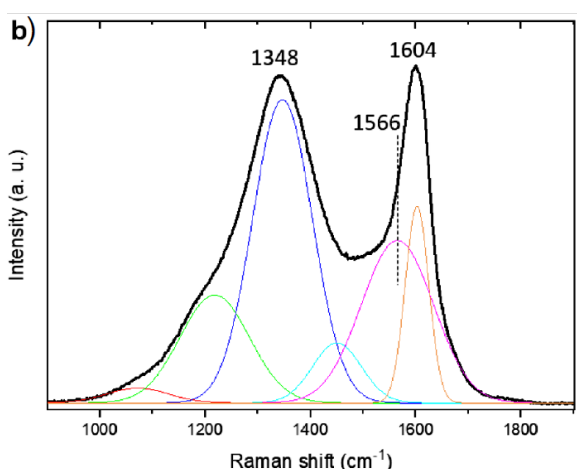


**Fig. 5.** Raman spectra and decomposition of C-ZTC (a) and CN-ZTC (b).

XPS analysis supports these findings (Fig. 6). The C1s peak for CN-ZTC is broader (FWHM = 1.8 eV) than that of



C-ZTC (0.9 eV), indicative of a more heterogeneous carbon environment. Its binding energy is also slightly higher (284.9 eV vs. 284.5 eV), suggesting increased sp³ content, in agreement with the Raman and elemental data. The C/N atomic ratio for CN-ZTC was found to be 12.8. Deconvolution of the N1s signal reveals contributions from pyridinic (24.2%), pyrrolic (8.5%), and graphitic nitrogen (49.4%), as well as minor peaks assigned to pyridinic-oxide and  $\pi$ - $\pi$ \* interactions. The CN-ZTC also has a significantly higher oxygen content (C/O = 8.2) compared to C-ZTC (C/O = 20.0), consistent with nitrogen-induced hydrophilicity.

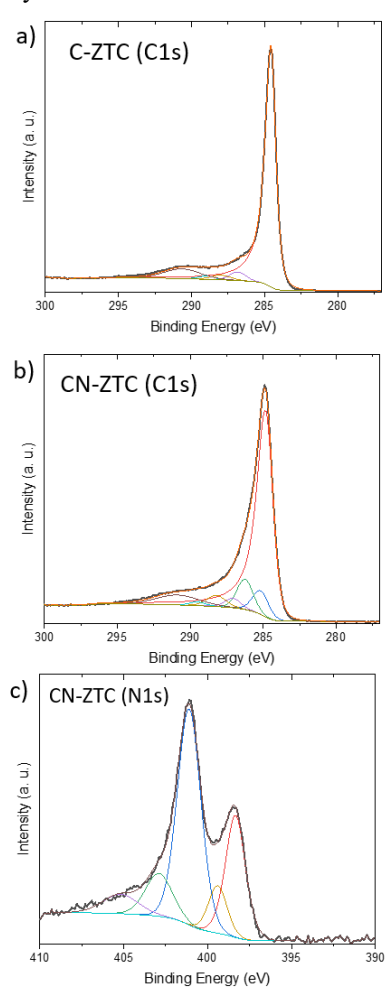


**Fig. 6.** X-ray C1s photoelectron peak of C-ZTC (a) and CN-ZTC (b). X-ray N1s photoelectron peak of CN-ZTC (c).

Electrochemical evaluation of ORR activity was conducted via rotating disk electrode voltammetry in the 1.0–0.2 V range. Polarization curves at 1600 rpm for C-ZTC, CN-ZTC, and commercial Pt/C are shown in Fig. 7a. Capacitive currents were subtracted using measurements in nitrogen-saturated electrolytes. Both ZTC-based catalysts show notable ORR activity, linked to their high surface areas (Table 1), but CN-ZTC demonstrates superior



performance with a half-wave potential of 0.81 V vs. RHE, close to that of Pt/C (0.86 V). These results outperform many N-doped graphenes and are comparable to biomass-derived N-doped carbons.

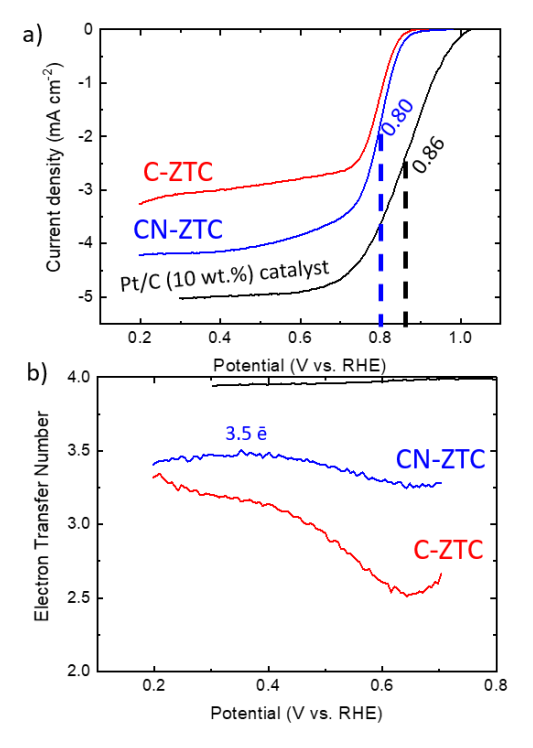


**Fig. 7.** (a) Linear sweep voltammetry (LSV) curves obtained for C-ZTC (red), CN-ZTC (blue), and the reference Pt/C catalyst (black) in an oxygen-saturated 0.1 mol  $L^{-1}$  KOH electrolyte, recorded at a rotation speed of 1600 rpm and a scan rate of 5 mV s<sup>-1</sup>; (b) Number of electrons transferred per O<sub>2</sub> molecule as a function of the applied electrode potential for C-ZTC (red), CN-ZTC (blue), and Pt/C (black) catalysts.

The enhanced performance of CN-ZTC is attributed to its higher nitrogen content and improved electrical conductivity, rather than surface area or structural order. The predominance of pyridinic and graphitic nitrogen species, both known to promote ORR, further supports its catalytic efficiency. Pyridinic nitrogen introduces Lewis base sites that facilitate O2 adsorption and reduction, while graphitic nitrogen modulates electron density on adjacent carbon atoms, enhancing charge transfer. The number of electrons transferred (n) during ORR is shown as a function of potential in Fig. 7b. C-ZTC exhibits a potentialdependent decrease in n from 3.5 to 2.5, indicating a mix of two- and four-electron pathways. In contrast, CN-ZTC maintains a nearly constant  $n \approx 3.5$ , suggesting a dominant four-electron mechanism and thus higher selectivity for hydroxyl production, which is crucial for efficient fuel cell operation.



# Conclusions

This study demonstrates that the use of pure acetonitrile as a carbon and nitrogen source enables the synthesis of nitrogen-rich zeolite-templated carbons (CN-ZTCs) with substantial heteroatom incorporation. Despite exhibiting morphological and structural features comparable to the ethylene-derived C-ZTC, the CN-ZTC displays markedly different physicochemical characteristics. The reduced microporosity of CN-ZTC is attributed to the formation of graphene-like carbon domains on the external surface of the particles. These modifications result in a less condensed carbon framework and significantly enhanced electrical conductivity. Most notably, the CN-ZTC exhibits superior oxygen reduction reaction (ORR) performance, achieving a high half-wave potential and excellent selectivity toward hydroxyl formation. These findings highlight the critical role of nitrogen doping and synthetic control in tailoring the electronic and catalytic properties of ZTCs. By fine-tuning synthesis parameters, it is possible to design efficient metalfree electrocatalysts, offering a promising route for nextgeneration energy conversion technologies.

# Acknowledgments

The authors gratefully acknowledge financial support from the European Union (ERDF) and the CAPES-COFECUB program under grant number 45020TE. The authors also thank the IC2MP (Institut de Chimie des Milieux et Matériaux de Poitiers) for providing research infrastructure and valuable technical support, as well as the Labpemol (Laboratório de Peneiras Moleculares) for personal assistance and collaborative input throughout this work.

## References

- 1. H. Nishihara, T. Kyotani, Zeolite-templated carbons three-dimensional microporous graphene frameworks, Chem. Commun. 54 (2018) 5648–5673.
- 2. T. Aumond, M. Esteves, Y. Pouilloux, R. Faccio, A. Sachse, Impact of the crystal size of beta zeolite on the structural quality of Zeolite Templated Carbons, Microporous Mesoporous Mater. 331 (2022), 111644.
- 3. X. Tong, X. Zhan, D. Rawach, Z. Chen, G. Zhang, S. Sun, Low-dimensional catalysts for oxygen reduction reaction, Prog. Nat. Sci. Mater. Int. 30 (2020) 787–795.
- 4. L.M. Rivera, G. García, E. Pastor, Novel graphene materials for the oxygen reduction reaction, Curr. Opin. Electrochem. 9 (2018) 233–239.
- J. Quílez-Bermejo, M. Melle-Franco, E. San-Fabi'an, E. Morall'on, D. Cazorla- Amor'os, Towards understanding the active sites for the ORR in N-doped carbon materials through fine-tuning of nitrogen functionalities: an experimental and computational approach, J. Mater. Chem. A 7 (2019) 24239–24250.